Formation of weakly bound, ordered adlayers of CO on rutile TiO_2(110): A combined experimental and theoretical study

M. Kunat,[1] F. Traeger,[1] D. Silber,[1] H. Qiu,[1] Y. Wang,[1] A. C. van Veen,[2] Ch. Wöll,[1,a)]
P. M. Kowalski,[3] B. Meyer,[3,4] C. Hättig,[3] and D. Marx[3]
[1]*Lehrstuhl für Physikalische Chemie I, Ruhr-Universität Bochum, 44780 Bochum, Germany*
[2]*Lehrstuhl für Technische Chemie, Ruhr-Universität Bochum, 44780 Bochum, Germany*
[3]*Lehrstuhl für Theoretische Chemie, Ruhr-Universität Bochum, 44780 Bochum, Germany*
[4]*Interdisziplinäres Zentrum für Molekulare Materialien (ICMM) and Computer-Chemie-Centrum (CCC), Universität Erlangen-Nürnberg, 91052 Erlangen, Germany*

(Received 11 December 2008; accepted 23 February 2009; published online 9 April 2009)

The adsorption of CO on the rutile TiO_2(110) surface was investigated using He atom scattering (HAS), high resolution electron energy loss spectroscopy (HREELS), thermal desorption spectroscopy (TDS), and different types of *ab initio* electronic structure calculations. The experimental and theoretical results allow to put forward a consistent picture for this rather complicated adsorbate system. At 70 K a (2×1) adlayer with a glide symmetry plane is formed, containing two molecules per unit cell which are tilted in alternate directions by about 20° relative to the surface normal. For this high density phase, the theoretical calculations reveal a substantial repulsion between CO molecules on neighboring lattice sites, in accord with the results of a detailed analysis of the experimental TDS data. The CO binding energy depends strongly on coverage and varies between 0.20 eV for the saturated monolayer and 0.36 eV for isolated molecules. The CO–CO repulsion leads to the desorption of about half of the CO molecules above 70 K and the formation of low density phases. HAS gave no indication of ordered adlayers at these lower coverages. For the internal stretching vibration of the CO molecules a value of 273 meV was determined by HREELS, in very good agreement with the theoretical calculations. © *2009 American Institute of Physics*. [DOI: 10.1063/1.3098318]

I. INTRODUCTION

With regard to chemisorption on metal surfaces, carbon monoxide is the molecular adsorbate for which the most experimental investigations have been published. For CO adsorbed on metal surfaces, a rather large variety of different structures has been observed experimentally[1] and analyzed on the basis of wave-function-based methods[2] and density functional theory (DFT).[3] As a result of repulsive interactions between adsorbed CO molecules, frequently rather open structures with large unit cells are observed at low coverages which convert to more densely packed phases at higher coverages.[1] A different situation is encountered for metal oxide single crystals. Here, the information available for adsorbed CO is rather scarce. Whereas IR spectroscopy carried out for metal oxide powders has been able to demonstrate that CO adsorbs on oxide surfaces with small- to medium-range binding energies, only very few detailed studies on oxide single crystal surfaces have been reported. The most detailed IR spectroscopy investigations were published for the cleaved MgO(001) surface.[4–6] In the case of the other most important vibrational spectroscopy, high resolution electron energy loss spectroscopy (HREELS), a few more studies are available, including ZnO (for a review, see Ref. 7). To our knowledge there is only one fairly recent report on the stretch frequency for CO adsorbed on rutile TiO_2(110).[8]

Most of the previous studies reported for CO adsorbed on oxide single crystal surfaces have focused on the determination of binding energies using thermal desorption spectroscopy (TDS) and spectroscopic studies using XPS or UPS. In particular, the lateral structures of CO adlayers on well-defined oxide surface are largely unknown. There is neither information about ordered phases at high coverages nor about high-order commensurate structures at lower coverage. This is an unfortunate situation, since more precise information on the adsorption of CO at oxide surfaces is required for a better understanding of catalytic processes involving CO, either as reactant or as a possible catalyst poison, e.g., in the case of methanol synthesis on ZnO (Ref. 9) or CO oxidation on the Au/TiO_2 system.[10,11] Previous work for CO adsorption on ZnO has shown that CO can also be used as a probe molecule to distinguish between different possible geometries of an oxide surface, see Refs. 12–14 for the case of the polar O-terminated ZnO surface.

In the case of titania, the oxide surfaces which have so far received the most attention (for a recent review, see Ref. 15), we are not aware of any experimental work on the structure of CO overlayers formed on any surface of the three different TiO_2 modifications (rutile, anatase, and brookite). Most experimental studies on the interaction of CO with titania have been carried out for anatase and rutile powders using IR spectroscopy.[16–23] The first IR study on CO adsorbates on the rutile TiO_2(110) single crystal surface has became available only very recently.[8] In all studies

a)Electronic mail: woell@pc.ruhr-uni-bochum.de.

 © 2009 American Institute of Physics

Downloaded 03 Nov 2010 to 134.147.252.238. Redistribution subject to AIP license or copyright; see http://jcp.aip.org/about/rights_and_permissions

consistently an intense adsorption band centered around 2183–2193 cm^{-1} has been reported (corresponding to a blueshift of the CO vibrational frequency of 40–50 cm^{-1} with respect to the gas phase value), which was attributed to CO bound to fivefold coordinated Ti sites. In the first TDS measurement a CO adsorption energy of 0.8 eV was obtained after adsorbing CO at room temperature on single crystal TiO_2(110) surfaces.[24] In a subsequent study on oxidized Ti foils, in which CO was adsorbed at 150 K, a much lower CO binding energy between 0.46 and 0.51 eV (44–49 kJ/mol, desorption peak around 200 K), depending on the annealing of the sample, was found.[25] However, from more recent TDS measurements on single crystal TiO_2(110) surfaces,[26–28] it became clear that the CO adsorption energies from these early studies have to be attributed to CO bound to defect sites and not to ideal parts of TiO_2 surfaces. Furthermore, Refs. 26–28 provided indirect evidence for the presence of repulsive lateral interactions between CO molecules on the TiO_2(110) surface. Linsebigler *et al.*[26,27] adsorbed CO at 105 K. The desorption maximum shifted from about 135 to 170 K with decreasing CO coverage. For the limit of zero coverage a CO binding energy of 0.43 eV (9.9 kcal/mol, using a pre-exponential factor of 10^{14} s^{-1}) was deduced. The shift in the desorption maximum was attributed to a repulsive lateral interaction between the CO molecules. A fit to the leading edge of the TD spectra yielded a repulsion energy of 0.10 eV (2.2 kcal/mol) at the maximum CO coverage, which was estimated to be 0.68 ML by assuming a CO sticking probability of 1. The CO binding energy at this maximum coverage thus corresponds to 0.33 eV. Dohnálek *et al.*[28] measured a sticking coefficient of about 0.8 which is almost independent of CO coverage. It is therefore likely that Linsebigler *et al.* have slightly overestimated their maximum coverage. For a sticking probability of 0.8, one obtains 0.5 ML instead of 0.68 ML. By adsorbing CO at a surface temperature of 32 K, Dohnálek *et al.* were able to saturate the TiO_2(110) surface with more than 1 ML of CO. From their TD spectra they obtained CO binding energies of 0.198 eV (19.1 kJ/mol), 0.348 eV (33.6 kJ/mol), and 0.44 eV (42 kJ/mol) for 1 ML, 0.5 ML, and in the limit of zero CO coverage, respectively, based on a frequency factor of 10^{13} s^{-1}.

Several groups have performed theoretical studies on the adsorption of CO on TiO_2(110) using different kinds of first-principles approaches.[29–35] The calculations agree that the CO molecules preferentially adsorb perpendicular to the surface at the fivefold coordinated Ti sites with a C-down orientation. A detailed analysis of the chemical bond showed that the CO bond strength is mainly determined by the CO polarization and the CO σ-donation to the surface, while the electrostatic attraction is almost exactly canceled by the Pauli repulsion.[31] Furthermore, all calculations using periodic boundary conditions found a strong repulsive interaction between the CO molecules in the monolayer coverage regime with a repulsion energy E_{rep} per CO molecule between 0.20 eV (Hartree–Fock[30,31]) and 0.13 eV [DFT (Ref. 33)]. However, the calculated CO binding energies vary widely between the calculations, from 0.29 to 0.8 eV for single CO molecules[29,31,32,34] and from 0.25 to 0.55 eV in the full monolayer coverage limit.[30–33,35] Also for the shift $\Delta\nu$ of the CO stretch frequency values between a blueshift of about +140 cm^{-1} and a redshift of −23 cm^{-1} have been reported.[31,33–35] There are several reasons for this wide scatter of results. In the early calculations only very small cluster models for the TiO_2(110) surface with no or insufficient embedding were used.[29,31] Some calculations are based on Hartree–Fock only,[29–32] therefore fully neglecting electron correlations, which typically results in an underestimation of the binding energy. On the other hand, adding correlations on the LDA level[32,35] leads to a large overestimation of the bond strength. The same is true, if conventional MP2 is used,[31] as we will show in the present study. In several calculations no relaxations of the atomic configurations were taken into account or only in a very limited fashion.[29–31,34] The TiO_2(110) surface, however, undergoes large surface relaxations[36–39] and rerelaxations upon adsorption can contribute 30% and more to the binding energy of molecules.[32,39] All periodic calculations were based on slabs with only three TiO_2 trilayers or less.[30–33,35] As noticed in several previous studies,[36,38,39] for TiO_2(110) the surface and molecular binding energies show large odd-even oscillations with the number of trilayers in the slab, and setups consisting of only three trilayers are usually not sufficient to get well converged results.

In the present paper we have studied the adsorption of CO on (110) oriented single crystal substrates of rutile TiO_2 using a number of different experimental and theoretical techniques. First, structural information on the CO adlayers was determined using helium atom scattering (HAS). In addition, we have obtained information on CO binding energies on the perfect parts of the surface using He-TDS.[40–42] In previous work it has been demonstrated that He-atom scattering is particularly well suited for the investigation of metal oxide surfaces and also TiO_2,[43] not only because of the fact that this technique is completely insensitive to any charging effects but also because of its pronounced sensitivity to small adsorbates such as H atoms and CO.[12,40] It should be noted that low energy electron diffraction (LEED), the standard technique used to determine the structure of CO adlayers on metal surfaces, cannot be used for the investigation of CO adlayers on oxide surfaces in a straightforward fashion since the excitations of electron hole pairs upon electron incident on the surface may lead to the desorption of CO molecules. For example, it is not possible to record XPS data for CO adlayers on the TiO_2 surface since the impinging photoelectrons lead to desorption of the molecules, similar to the case of H_2O adsorbed on Ru(0001).[44] In order to allow for a detailed comparison with the previous experimental data on single crystals,[26–28] we have also carried out measurements on both, perfect and defective TiO_2(110) surfaces, using conventional TDS. Since the shape of the TDS data indicated that a standard Redhead-type analysis is not appropriate, simulations of the TDS data were performed using the ASTEK program package,[45] which allowed to fit the binding energy per molecule at low coverage as well as the repulsion energy between neighboring CO molecules. In addition, CO adsorbates on TiO_2(110) have been studied by HREELS. Although this is a standard technique to study molecular vibrations of adsorbates on single crystal surfaces, systematic

Downloaded 03 Nov 2010 to 134.147.252.238. Redistribution subject to AIP license or copyright; see http://jcp.aip.org/about/rights_and_permissions

investigations employing vibrational spectroscopy of adsorbates on ZnO and TiO_2 single crystal surfaces have only recently been reported.[7,8,46,47] In the course of the present work the internal stretching frequency of CO on TiO_2(110) as well as the CO binding energy have been determined. Finally, detailed electronic structure calculations were carried out employing DFT and wave-function-based methods to determine the atomic structure, binding energy, and shift of vibrational stretch frequency of CO molecules, ranging from monolayer coverage to the limit of isolated molecules.

II. EXPERIMENTAL

The He-atom scattering apparatus used here has been described in detail previously.[48] Briefly, He gas is expanded through a small orifice, scattered from the substrate, and detected using a magnetic mass spectrometer. The total scattering angle of the He atoms (sum of incident and exit angles) is fixed, but the angle of incidence, θ_i, can be changed by rotating the sample around an axis normal to the scattering plane. In the scattering chamber also LEED and XPS are available. The HREELS and TDS experiments were performed in an ultrahigh vacuum (UHV) apparatus, consisting of two chambers separated by a valve.[49] The base pressure was 2×10^{-11} mbar in both chambers. The upper chamber was equipped with an argon ion sputtering gun, a LEED optics, and a quadrupole mass spectrometer for TDS experiments. The lower chamber housed a HREELS spectrometer of the latest Ibach design (Delta 0.5, SPECS Germany) with a straight-through energy resolution of 1 meV. HREEL spectra were recorded at an angle of incidence of 55° with respect to the surface normal in specular geometry. The energy of the primary electrons was set to 10 eV.

The TiO_2 substrates used in this study were obtained from MaTeck crystals and were cleaned by a procedure consisting of cycles of Ar^+ sputtering (600 V, ≈1 μA, $T_s=300$ K, 60 min) followed by annealing in oxygen (1×10^{-6} mbar, $T_s\approx600$ K, 10 min) and in UHV ($T_s=750$ K, 5 min), as described in previous publications (see Ref. 50). A NiCr/Ni thermocouple was tightly clamped against the side of the substrate. The crystal was never heated above 850 K in order to avoid an excessive loss of oxygen. The crystal exhibited a light blue color, revealing the presence of a small amount of oxygen vacancies in the bulk. After a few preparation cycles a sharp LEED pattern and a distinct He-atom specular peak revealed the presence of a structurally well-defined surface. XPS showed no carbon containing species (contamination level less than 0.05 ML) and symmetric Ti-2p peaks that are characteristic for a stoichiometric crystal.[24,50] The gases used in this study are of research purity (99.9999% for He, 99.999% for H_2, and 99.997% for CO). The crystal could be cooled down to a surface temperature T_s of approximately 50 K by means of liquid helium.

III. COMPUTATIONAL

The periodic DFT calculations for different configurations of CO adsorbed on the TiO_2(110) surface were carried out using the Car–Parrinello molecular dynamics program package CPMD.[51,52] The gradient-corrected Perdew–Burke–Ernzerhof (PBE) functional[53] and Vanderbilt ultrasoft pseudopotentials[54] were employed together with a plane wave basis set (cutoff energy of 30 Ry) to represent the Kohn–Sham orbitals. The optimized TiO_2 bulk lattice parameters were determined to be $a=4.649$ Å, $c=2.966$ Å, and $u=0.305$, which compares very well to the experiment values ($a=4.594$ Å, $c=2.959$ Å, and $u=0.305$, see Ref. 55).

For the study of "single" CO molecules, we used slabs with extended (4×2) surface unit cells, corresponding to a effective CO coverage of 1/8 ML in which the CO molecules are separated by almost 12 Å. The calculations for the higher CO coverages were done with the same surface unit cell which was gradually filled with up to eight CO molecules. The calculated bulk equilibrium lattice constants were used for the lateral extension of the slabs. Due to the large size of the supercell the k-point sampling could be restricted to the Γ-point. All configurations were relaxed by minimizing the atomic forces. Convergence was assumed when the largest component of the residual forces on the ions was less than 0.01 eV/Å. As we will show later on, very well converged results for the CO binding energy could be achieved by using a slab thickness of four TiO_2 trilayers of which only the atoms in the upper two trilayers were allowed to relax, whereas the bottom two trilayers were fixed at the bulk positions. Furthermore, the broken surface bonds of the fivefold coordinated Ti and the twofold bridging O atoms at the bottom of the slab were saturated[56] with hydrogenlike atoms of nucleus charges of +4/3 and +2/3, respectively (for more details, see Ref. 39). As shown in Ref. 39 with this setup also well converged results for the adsorption of hydrogen and water and the formation of vacancies on TiO_2(110) were obtained. The vacuum region between the periodically repeated slabs had a thickness of about 13 Å which corresponds to the thickness of the slab itself. Overall, this setup resulted in supercells containing in total 208 atoms, including the artificial atoms to saturate the broken surface bonds at the bottom of the slabs.

The vibrational frequencies of the CO molecules were obtained in harmonic approximation by a finite difference scheme. The C and O atoms were displaced by 0.01 Å in the x-, y-, and z-directions. For the isolated CO gas phase molecule we obtained a CO stretch frequency of 2144 cm^{-1} with our calculational setup which is almost identical to the (anharmonic) experimental value of 2143 cm^{-1}. Therefore, no scaling factor was applied to the calculated vibrational frequencies of the CO molecules adsorbed on the TiO_2(110) surfaces.

To account for nonlocal dynamical electron correlation effects—in particular, the van der Waals dispersion interaction—MP2 and SCS-MP2[57] calculations were carried out for a finite embbeded cluster model. Cutouts of 40 Ti and 80 O atoms around the adsorption site were embedded in a set of 217 Ti cationic cores modeled by effective core potentials (ECP 18 SDF potential for Ca taken from Ref. 58) and a two-dimensional eight layer thick periodic slab of point charges. Formal ionic charges of +4 and −2 have been used for the embedding, and the geometry of the TiO_2 slab was fixed at the results from the periodic DFT calculation for full

Downloaded 03 Nov 2010 to 134.147.252.238. Redistribution subject to AIP license or copyright; see http://jcp.aip.org/about/rights_and_permissions

monolayer coverage with CO. The geometry of the absorbed CO molecules was assumed to be upright with the equilibrium CO bond distance evaluated for the gas phase with the respective quantum-chemical method. Only the Ti–CO distance was reoptimized in the embedded cluster calculations.

The MP2 calculations were done with a doubly polarized valence triple zeta (TZVPP) basis[59] for the adsorbate (CO) and its next 14 Ti and O neighbors in the case of a single adsorbed CO molecule and the next 27 neighbors in the case of three adsorbed CO molecules. From the latter calculations, we estimated the MP2 corrections to the repulsion by the neighboring adsorbates that a CO molecule experiences at monolayer coverage. For all other atoms of the $Ti_{40}O_{80}$ cluster a polarized split valence (SVP) basis[60] was used. All embedded cluster calculations were corrected for basis set superposition errors using the full counterpoise correction of Boys and Bernardi[61] and were carried out with the TURBOMOLE (Ref. 62) program package. For the MP2 calculations we used the parallel RI-MP2 implementation reported in Ref. 63 with optimized auxiliary basis sets from Ref. 59. The same embedding scheme and basis sets, including the counterpoise correction, were used to carry out embedded cluster DFT/PBE calculations. The differences between embedded cluster DFT and MP2 calculations were then combined with the results from the periodic DFT calculations to obtain best theoretical estimates for the binding energies of CO on TiO_2.

IV. RESULTS

A. Experimental

In Fig. 1 we show a series of He atom angular distributions recorded for a substrate temperature of 70 K along the [001] high-symmetry direction. The data for the clean surface (on top) are fully consistent with previous LEED data[37] as well as with our previous results obtained for this surface[64] and indicate the presence of a perfect (1×1) rutile $TiO_2(110)$ surface. When the surface is exposed to CO the intensity of the specular signal as well as the intensity of the diffraction peaks change, demonstrating that CO adsorbs on the surface. The fact that the new diffraction peaks have the same widths as those seen for the clean surface reveals the formation of an ordered structure. No new diffraction peaks are observed along the [001] direction. Although this is indicative of the formation of a (1×1) overlayer, one should note that a possible half order diffraction peak may be extinguished because of a glide plane symmetry.[65] For the particular incident energy chosen in this set of experiments (32.6 meV), the first-order diffraction peaks were about seven times more intense than the specular peaks, whereas after saturation of the surface with CO (which occurs after an exposure to about 2.4 L), the specular peak is clearly more intense than the first-order diffraction peak. These data imply a fairly large sticking coefficient. In fact, a detailed report on the value of the sticking coefficient and the dependence of the sticking coefficient on incident energy obtained using the same apparatus has been published earlier.[66] A more detailed analysis of the diffraction peak intensities as a function of exposure to CO reveals a continuous change which saturates after an exposure of 2.4 L.

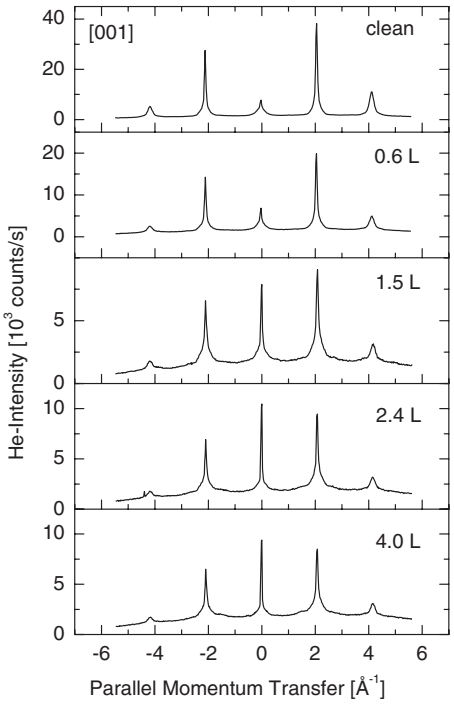


FIG. 1. Series of He atom angular distributions recorded for clean $TiO_2(110)$ at a substrate temperature of 70 K along the [001] high-symmetry direction (top) and for CO adsorbates after the exposure given in the figure (bottom). The incident wave vector of the He beam was 7.9 $Å^{-1}$ and the CO gas was applied at 9.5×10^{-9} mbar (corrected for ionization probability of 0.95 relative to N_2).

The data recorded along the other high-symmetry azimuthal direction, $[1\bar{1}0]$, are shown in Fig. 2. Also along this direction there is no indication of new diffraction peaks indicating an additional periodicity. As for the other azimuthal direction, a significant change in the relative diffraction intensities is observed upon exposure to CO, revealing the formation of an ordered adlayer. Note that the width of the diffraction peaks for saturation coverage along this azimuth

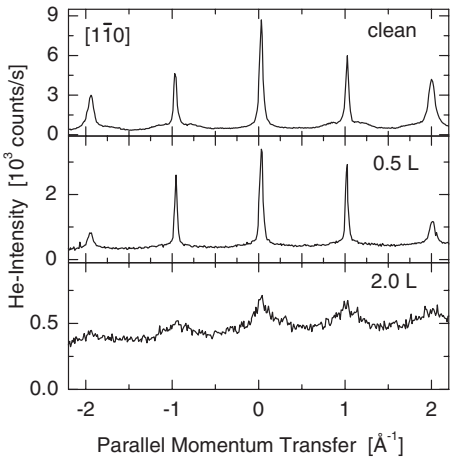


FIG. 2. He atom angular distributions for the clean $TiO_2(110)$ surface along the $[1\bar{1}0]$ high-symmetry direction and for two coverages of CO adsorbates after the exposure given in the figure. The surface temperature was between 74 and 65 K. The incident wave vector of the He beam was 4.8 $Å^{-1}$ and the CO gas was applied at $(9.5-7.6)\times10^{-8}$ mbar (corrected for ionization probability of 0.95 relative to N_2).

Downloaded 03 Nov 2010 to 134.147.252.238. Redistribution subject to AIP license or copyright; see http://jcp.aip.org/about/rights_and_permissions

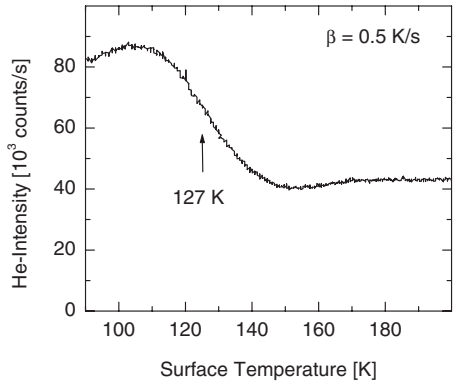


FIG. 3. He-TDS curve, i.e., specular intensity while heating the crystal. The first step at a desorption temperature of 127 K can be attributed to the CO adsorbate. The incident wave vector was k_i=7.9 Å^{-1}.

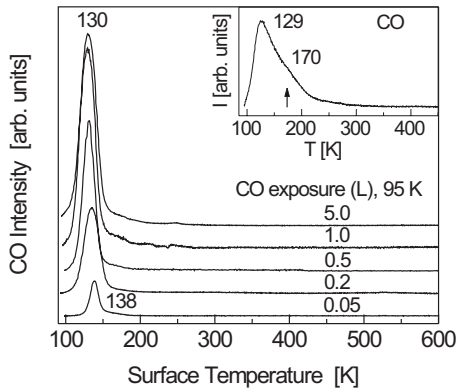


FIG. 4. TDS data of CO (mass 28) for various CO exposures on the perfect TiO_2(110) surface at 95 K. The inset shows the TD spectrum of CO after exposing the defective TiO_2(110) surface to 5 L CO at 95 K. The heating rate was 1.5 K/s.

is rather large. This observation has been reproduced several times and indicates a significant amount of disorder along this direction.

Altogether the He-atom angular diffraction scans clearly indicate the formation of a well-defined adlayer with well-defined peaks at integral order positions and without any superstructure peaks along the high-symmetry directions when the TiO_2 rutile (110) surface is exposed to CO at a temperature of 70 K.

In Fig. 3 we present He-TDS data which have been recorded by monitoring the intensity of the He-atom specular peak as a function of surface temperature. In previous work it has been demonstrated that by analyzing the temperature dependence of the He-atom specular peak intensity, information equivalent to conventional TDS can be obtained.[12,67] The major difference is the higher specificity of He-TDS: whereas in conventional TDS all desorbing molecules are detected, with He-TDS we are sensitive to CO molecules bound to the perfect parts of the surface only. The data shown in Fig. 3 reveal a pronounced change in the He-atom reflectivity at a surface temperature of 127 K, which can be unambiguously related to the desorption of CO molecules from the perfect parts of the TiO_2 substrate. The most obvious feature in the He-TDS data is the decrease in intensity, indicating a strong change in surface CO coverage. Assuming that the activation energy for desorption is equal to the binding energy of CO to the surface and by applying a standard Redhead analysis[68] with a frequency factor of 1×10^{13} s^{-1}, we obtain a binding energy of (340 ± 25) meV. This binding energy corresponds to the value for a coverage of approximately half a monolayer.[28] It should be noted that the decrease in intensity upon CO desorption is a result of the particular incident energy chosen in these experiments. At other incident energies the opposite behavior, i.e., an increase in the reflectivity can be observed.

Figure 4 displays the TDS data of CO (mass of 28 u) on the perfect TiO_2(110) surface after exposure to CO at 95 K. For very low exposure (0.05 L) the desorption maximum is found at 138 K. With increasing the CO exposure, the desorption peak shifts slightly to lower temperatures and is observed at 130 K at saturation. It corresponds to a CO binding energy of 0.343 eV when assuming a frequency factor of 1×10^{13} s^{-1} in first-order kinetics, in good agreement with the He-TDS results.

The adsorption of CO on TiO_2(110) is also clearly identified by vibrational spectroscopy. The HREELS data of the clean as well as CO adsorbed TiO_2(110) surfaces are presented in Fig. 5. The raw spectrum of the clean surface is dominated by the intense primary Fuchs–Kliewer phonons at 45, 55, and 94 meV as well as their combination modes (curve a). The latter have been nearly completely removed by the Fourier deconvolution process, which makes it possible to detect the vibrational frequencies of adsorbates (curve b). After exposing TiO_2(110) to 10 L CO at 95 K, a new loss at 273 meV (2200 cm^{-1}) is observed in the deconvoluted spectrum (curve c). It is characteristic of the presence of CO on the TiO_2(110) surface and attributed to the internal CO stretching mode. The frequency is rather similar to that observed very recently using IR spectroscopy for CO adsorbed on the same surface (2190 cm^{-1} in the low CO coverage limit, see Ref. 8). Also, the frequency is rather similar to the corresponding species observed on the mixed-terminated ZnO$(10\bar{1}0)$ surface.[69–71]

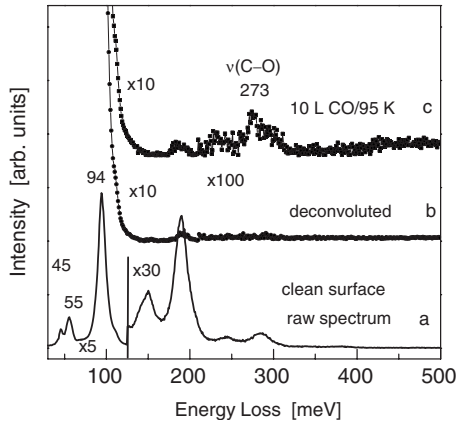


FIG. 5. HREELS spectra recorded for the clean TiO_2(110) surface (curves a and b) and after exposure to 10 L CO at 95 K (curve c). Curve a displays the raw spectrum, and the Fourier-deconvoluted spectra are shown in curves b and c. The spectra were recorded at 95 K in specular direction with an incidence angle of 55° and with a primary energy of 10 eV.

Downloaded 03 Nov 2010 to 134.147.252.238. Redistribution subject to AIP license or copyright; see http://jcp.aip.org/about/rights_and_permissions

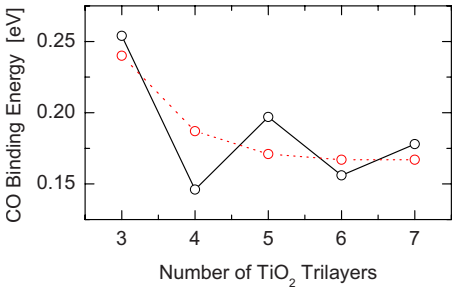


FIG. 6. (Color online) Convergence of the CO adsorption energy E_{ad} with slab thickness at full monolayer coverage. The results for full atomic relaxation with CO adsorbed symmetrically on both sides of the slab are shown by a solid black line. The dashed red line represents the calculations in which CO was adsorbed only on one side of the slab with the bottom two trilayers fixed at the bulk positions and the broken surface bonds at the bottom of the slab saturated with pseudohydrogen atoms.

B. Theoretical

For the periodic DFT calculations we first checked carefully how thick we have to choose our slabs in order to get well converged results for the CO binding energies. In a first set of calculations a full monolayer of CO was adsorbed symmetrically on both sides of the slabs with the CO molecules sitting in an upright position above the fivefold coordinated Ti surface sites with the carbon atom binding to the Ti. A full geometry optimization was performed, allowing all atoms in the slab to relax. The orientation of the CO molecules, however, was enforced to an upright orientation by keeping the two mirror symmetry planes of the $TiO_2(110)$ surface. The calculated CO binding energies E_{ad} for different slab thicknesses are shown in Fig. 6. Strong odd-even oscillations can be seen which are well known also from calculations of the surface energy as well as vacancy formation and adsorption energies of other molecules (see Ref. 39 and reference therein). In the calculations with slabs of a thickness of three trilayer E_{ad} is overestimated by about 0.1 eV. Altogether, quite thick slabs are needed to get a well converged CO binding energy. In a second set of calculations, the CO monolayer was adsorbed only on the top side of the slab. At the bottom, the broken surface bonds were saturated with hydrogenlike atoms as described in the method section, and the bottom two trilayers were fixed at their bulk positions in the atomic relaxation. Again, the CO molecule was restricted to an upright orientation. Figure 6 shows that with this setup, the odd-even oscillations are almost completely eliminated and well converged results within an accuracy of 0.02 eV for E_{ad} are already obtained for a slab thickness of four trilayers. Therefore, this setup was chosen for all subsequent calculations.

For a single CO molecule in the (4×2) surface unit cell of our slab, we find that the upright position above the fivefold coordinated Ti sites remains the preferential adsorption geometry even without enforcing symmetry. Compared to the gas phase value the CO stretching frequency is blueshifted by 50 cm^{-1} or 6 meV, and an adsorption energy of 0.323 eV is obtained at the DFT/PBE level (see Table I). For a full CO monolayer the binding energy drops to 0.188 eV if the adsorption geometry is constraint to an upright orientation. There is thus a large lateral interaction between CO molecules adsorbed at neighboring sites. As a consequence the blueshift of the CO stretch frequencies decreases to 32 cm^{-1} or 4 meV. An unconstrained optimization of the adsorption geometry, however, reveals that an all upright configuration is not the optimal structure at a 1 ML CO coverage. An alternating tilting of the CO molecules by about 20° out of the vertical position reduces the repulsive lateral interaction at 1 ML coverage from 0.135 to 0.122 eV per CO molecule (see Table I). The final structure has a (2×1) periodicity with a glide symmetry plane along the [001] direction (see Fig. 7). A very similar situation was observed for CO adsorbed on Ni(110).[72,73] The lateral repulsion between CO molecules is only present if neighboring lattice sites are occupied. A (2×1) arrangement of 1/2 ML of CO molecules in which every second lattice site along the [001] direction remains empty gives basically the same results as for the single CO molecule within the accuracy of the periodic DFT/PBE calculations. In particular, the coupling between CO molecules in different [001]-rows is negligible. Taking the fully relaxed structure of CO on $TiO_2(110)$ in the monolayer coverage regime and flipping the orientation of the tilted CO molecules in every second [001]-row (which leads to a (2×2) periodicity of the CO layer, see Fig. 8) results in a CO binding energy which is only reduced by 3 meV. Thus, no pronounced ordering of the CO adsorbate layer in the $[1\bar{1}0]$-direction can be expected.

TABLE I. Results of the periodic DFT/PBE calculations for the adsorption energy E_{ad} (in eV) of CO on $TiO_2(110)$ and the frequency shift $\Delta\nu$ (in cm^{-1}) for the CO stretch mode.

CO coverage	E_{ad}	$\Delta\nu$
Single CO	0.323	50
Monolayer CO (upright)	0.188	32
Monolayer CO (tilted)	0.209	

The embedded cluster Møller–Plesset perturbation theory calculations give significantly larger binding energies for CO on the $TiO_2(110)$ surface (see Table II) of 0.740 eV with MP2 and 0.646 eV with SCS-MP2. SCS-MP2 includes an empirical correction for the usual overestimation of correlation effects at the MP2 level[74] and therefore usually gives more reliable results for adsorption energies than MP2. The finite size of the cluster in these calculations leads to an overestimation of the ionicity and thereby of the CO binding

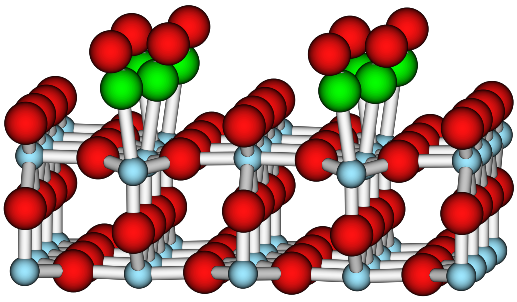


FIG. 7. (Color online) Fully relaxed atomic structure of a CO monolayer adsorbed on $TiO_2(110)$. C, O, and Ti atoms are shown in green, red, and gray, respectively.

Downloaded 03 Nov 2010 to 134.147.252.238. Redistribution subject to AIP license or copyright; see http://jcp.aip.org/about/rights_and_permissions

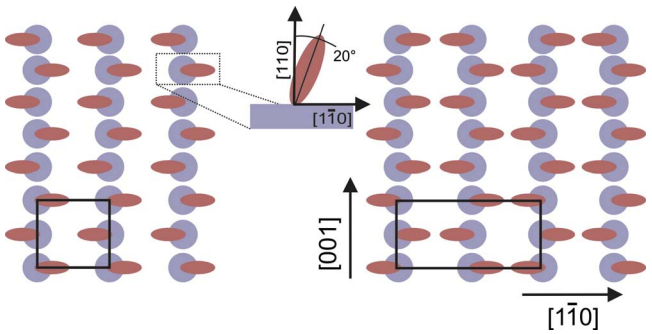


FIG. 8. (Color online) Schematic sketch of the orientation of the CO molecules in a monolayer adlayer with (left) a (2×1) and (right) a (2×2) periodicity, both containing glide mirror planes.

energies.[32] To correct for this and the error caused by an incomplete structure optimization at the MP2 level, we only take the difference between the DFT/PBE and the MP2 (or SCS-MP2) results from the embedded cluster calculations as a correction for the periodic DFT values. These corrections account mainly for the attractive van der Waals dispersion interaction between CO and the rutile surface or between CO molecules at neighboring adsorption sites and other nonlocal electron correlation effects which are not accounted for by the PBE functional. With MP2 we obtain for this correction 0.186 eV and with SCS-MP2 0.092 eV, which reflects the fact that MP2 usually overestimates somewhat electron correlation effects. Similarly we obtain for the repulsive lateral interaction in a CO monolayer correction of +14 meV (MP2) and +48 meV (SCS-MP2). Combining the results from the periodic DFT/PBE calculations with the MP2 or SCS-MP2 corrections to DFT/PBE from the embbeded cluster calculations and the zero-point vibrational correction (ZPVC) of −51 meV, we arrive at best estimates for the binding energies of a single CO molecule on the rutile surface of 0.458 eV (MP2) and 0.364 eV (SCS-MP2), see Table III. In a similar way we obtained for the repulsive lateral interaction E_{rep} in a CO monolayer best estimates of 0.128 eV (MP2) and 0.162 eV (SCS-MP2) per CO molecule. Thus, the lateral interaction leads to a strong decrease in the adsorption energy in a full monolayer with E_{ad} of 0.330 eV (MP2) and 0.202 eV (SCS-MP2), see Table IV. Since an overestimation of the electron correlation effects is often observed in normal MP2 (i.e., without SCS corrections),[74] we take the best estimates for E_{ad} and E_{rep} from the SCS-MP2 calculations as our final result, i.e., 0.36 eV for the adsorption energy for noninteracting CO molecules and 0.20 eV at full monolayer coverage which corresponds to a CO–CO repulsion energy of 0.16 eV (rounded to a precision of two significant digits).

TABLE II. Results for the adsorption energy E_{ad} (in eV) of CO on TiO_2(110) and the lateral CO–CO repulsion energy E_{rep} (in eV) for CO molecules in a full CO monolayer from embedded cluster Hartree–Fock, MP2, SCS-MP2, and DFT/PBE calculations, and the ZPVC (in eV) evaluated at the DFT/PBE level.

Method	Single CO	1 ML CO	E_{rep}
Hartee–Fock	0.341	0.017	0.324
DFT/PBE	0.554	0.304	0.150
MP2	0.740	0.576	0.164
SCS-MP2	0.646	0.450	0.198
ZPVC	−0.051		

TABLE III. Best estimates obtained from the periodic DFT/PBE and the embedded cluster MP2 calculations for the adsorption energy E_{ad} (in eV) of a single CO molecule adsorbed on TiO_2(110).

	MP2		SCS-MP2
Periodic DFT/PBE		+0.323	
ZPVC		−0.051	
Embedded cluster (SCS-)MP2–DFT	+0.186		+0.092
Best estimates for E_{ad} for iso CO	+0.458		+0.364

V. DISCUSSION

The present as well as previous theoretical calculations[30–33] of the coverage dependent CO binding energy reveal the presence of a significant repulsion between CO molecules on neighboring lattice sites of the rutile TiO_2(110) surface. The binding energy drops from 0.36 eV for an isolated molecule to 0.20 eV for CO in a densely packed monolayer. To analyze the impact of such a rather strong repulsive interaction on the experimental thermal desorption data, we have carried out TDS simulations using the ASTEK program package.[45] The ASTEK simulations are based on a lattice gas Hamiltonian in which the special symmetry of the substrate as well as the interactions between neighboring adsorbate molecules are explicitly taken into account. This lattice gas Hamiltonian is then used to solve the rate equation for the desorption of the adsorbate molecules in a mean field approximation.

In our simulations for each CO binding site only an on-site adsorption energy term E_{ad} and a repulsive interaction E_{rep} to the two nearest neighbors along the [001]-directions were considered. Using the results of the theoretical analysis of E_{ad}=0.36 eV and E_{rep}=0.16 eV, we find for initial coverages of full CO monolayers that a first desorption peak evolves around 75 K. This is in full agreement with the TDS measurements by Dohnálek *et al.*,[28] in which a CO monolayer coverage could be achieved by adsorbing CO at a temperature of 32 K. From an inversion analysis of their TD spectra (using a frequency factor of 10^{13} s^{-1} and a heating rate of 1 K/s) they obtained a CO binding energy at 1 ML coverage of 0.198 eV which matches excellently our calculated value of 0.20 eV.

TABLE IV. Best estimates for the lateral repulsion energy E_{rep} (in eV) for a CO molecule in a full CO monolayer (taken with respect to E_{ad} for a single CO and the adsorption energy per CO molecule in a full monolayer).

	MP2		SCS-MP2
Periodic DFT/PBE (upright)		+0.135	
Periodic DFT/PBE (tilted)		−0.021	
Embedded Cluster (SCS-)MP2–DFT	+0.014		+0.048
Best estimates for E_{rep}	+0.128		+0.162
Best estimates for E_{ad} for iso CO	+0.458		+0.364
Best estimates for E_{ad} for CO in ML	+0.330		+0.202

Downloaded 03 Nov 2010 to 134.147.252.238. Redistribution subject to AIP license or copyright; see http://jcp.aip.org/about/rights_and_permissions

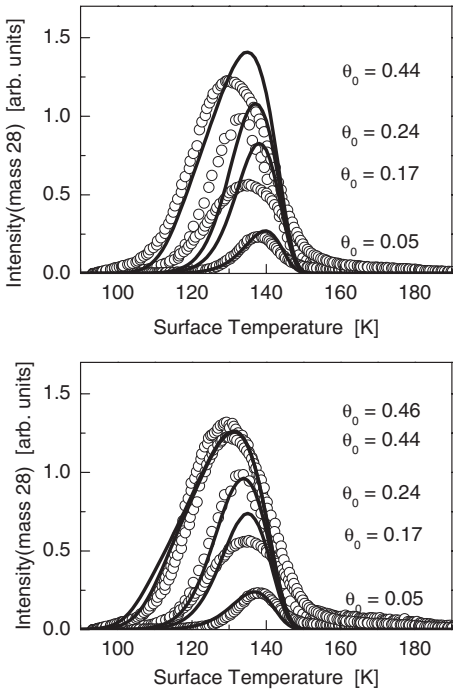


FIG. 9. Comparison of the experimentally observed (open circles) and the simulated (lines) TD spectra for (top) a parameter set of E_{ad}=0.36 eV and E_{rep}=0.16 eV as taken from the theoretical predictions and a fitted frequency factor of 4×10^{11} s^{-1} and (bottom) the best fitting parameter set with E_{ad}=0.31 eV, E_{rep}=0.16 eV, and a frequency factor of 9.9×10^{11} s^{-1}.

In the temperature range above 95 K, where our TDS measurements were carried out, about half of the CO molecules are desorbed. Therefore, all further ASTEK simulations were done by starting from 0.5 ML coverages and less with a random distribution of the CO molecules. Figure 9(a) shows that a very reasonable fit of the experimental TDS data is obtained when using our theoretical values for E_{ad} and E_{rep} and a frequency factor of 4×10^{11} s^{-1}. The agreement between the simulated TDS curves and the experimental data can be further improved by not only fitting the frequency factor but also the CO binding energy E_{ad} while keeping the CO–CO repulsion E_{rep} at the theoretical value of 0.16 eV [see Fig. 9(b)]. This procedure yielded values of 9.9×10^{10} s^{-1} and E_{ad}=0.31 eV.

Overall, the experimental data and the theoretical calculations show a very consistent picture. The desorption maximum of 130 K in the TDS experiment and TDS simulations coincides nicely with the maximum in the change in the He-atom reflectivity in He-TDS at 127 K and also matches the desorption maxima of 130 and 135 K in the TDS measurements for about 0.5 ML CO coverages reported by Linsebigler *et al.*[26,27] and Dohnálek *et al.*,[28] respectively. Thus, the CO binding energies of 0.343 and 0.340 ± 0.025 eV obtained by a simple Redhead analysis of our TDS and He-TDS data, respectively, agree excellently with the binding energy of 0.33 eV reported by Linsebigler *et al.*[26,27] for their maximum coverage (about 0.5 ML) and the binding energy of 0.348 eV obtained by Dohnálek *et al.*[28] for 0.5 ML by an inversion of their TD spectra. These values, in turn, are very close to our calculated CO binding energy of 0.36 eV for single CO molecules, which is almost identical to the binding energy we get if we assume a 0.5 ML coverage and leave every second adsorption site along the [001] direction empty.

There is, however, a significant discrepancy between our data and the results from Linsebigler *et al.*[26,27] and Dohnálek *et al.*[28] when we go to lower CO coverages. Both report significant shifts of the desorption temperature maximum to higher values if the CO coverage is lowered beyond 0.5 ML. Consequently, at lower coverages their TD spectra extend to higher temperatures and show pronounced tails up to about 170 K. Thus, in both studies it is concluded that there is still an appreciable repulsive interaction between the CO molecules even at coverages below 0.5 ML. This is quantified in the CO binding energies in the limit of zero coverage of 0.43 eV (Refs. 26 and 27) and 0.44 eV (Ref. 28) which they deduce from their TDS data.

This behavior is not supported by our data. Figure 4 shows that the desorption maximum in our TD spectra only shifts from 130 to 138 K at low CO exposures and no CO desorption at temperatures above 150 K is detected. This is in accord with our periodic DFT calculations in which only a negligible small repulsion between CO molecules beyond the nearest-neighbor distance was found. On the basis of only nearest-neighbor repulsion, however, we were not able to obtain for any set of parameters in the ASTEK simulations high temperature TDS tails reaching up to 170 K. On the contrary, the largest deviation between the experimental TDS data and the predicted curves from ASTEK for our best set of parameters occurs in the high temperature tail where beyond 140 K the simulated curves are systematically lower than the experimental intensities [see Fig. 9(b)]. Also the inspection of the He-TDS data (see Fig. 3) gives no indication for CO species adsorbed on the perfect parts of the TiO_2(110) surface beyond 150 K. In this context it should be noted that with He-TDS, not the desorption of the CO molecules itself but the reappearance of well ordered areas on the clean substrate is determined.[67]

This apparent inconsistency between our results and those of the previous TDS studies by Linsebigler *et al.*[26,27] and Dohnálek *et al.*[28] can be resolved by assuming that the CO molecules desorbing in the high temperature tails beyond 150 K were actually bound to defect sites of the TiO_2 substrate, e.g., steps or vacancies. To corroborate our conclusion we have prepared a defective TiO_2(110) surface by Ar^+ ion sputtering which creates many defect sites (in particular, O vacancies) on the surface.[46] When this modified surface is subsequently exposed to CO at 95 K, the corresponding TD spectrum shows a clear shoulder centered at about 170 K in the high temperature side, revealing the adsorption of CO at defect sites (see inset of Fig. 4).

The experimental value for the CO vibrational frequency of 273 meV (2200 cm^{-1}) from the HREELS measurement supports that the CO molecules are bound via the carbon atom to the fivefold coordinated Ti sites on the TiO_2(110) surface, as schematically depicted in Fig. 7 (see Ref. 31 for a detailed analysis). The theoretical result for the CO stretch frequency from the periodic DFT calculations amounts to 2194 cm^{-1} at low coverage and 2176 cm^{-1} at a saturated monolayer, corresponding to blueshifts (with respect to the

Downloaded 03 Nov 2010 to 134.147.252.238. Redistribution subject to AIP license or copyright; see http://jcp.aip.org/about/rights_and_permissions

theoretical gas phase value) of 50 and 32 cm^{-1}, respectively. This is in full agreement with the present HREELS result and the results of a previous IR study[8] where frequencies of 2190 cm^{-1} (blueshift of 47 cm^{-1}) at low coverage and 2183 cm^{-1} (blueshift of 40 cm^{-1}) at higher coverage were observed. The frequency shifts are also very similar to those reported for various TiO_2 powders.[16–23]

At this point we can conclude that the agreement between the theoretical calculations for CO at low coverages and at high coverages with the experimental TDS is very satisfying. We now turn to the question of the lateral structure of the adsorbed CO adlayer. In the case of metal surfaces, the presence of strongly repulsive interactions between adsorbates typically leads to the formation of higher order superstructures at low coverages.[3] On the MgO(001) cleavage face, depending on CO coverage, two different structures have been found.[4–6] The unit cell of the more dense $c(4\times2)$ phase, for example, contains alternately, upright and tilted CO molecules. On this rather weakly corrugated oxide surface extensive long-range ordering has been observed by HAS.

In the case of CO/TiO_2(110), despite substantial efforts, no superstructure diffraction peaks could be observed in the HAS data along the two high-symmetry directions, [001] and $[1\bar{1}0]$. In the case of the rather anisotropic rutile TiO_2(110) surface, one would expect that such less densely packed structures occur first along the [001]-azimuth, where the distance between adjacent CO adsorption sites amounts to 2.96 Å, in contrast to 6.49 Å along the other high-symmetry direction $[1\bar{1}0]$. In none of our angular distributions we were, however, able to observe additional higher order diffraction peaks which would indicate the presence of such lower coverage phases. We propose that the absence of such low density ordered structures results from the fairly large activation energy for diffusion of CO adsorbed on this metal oxide surface. A large barrier for diffusion would yield to a random pattern of adsorbed CO molecules (note that the sticking coefficient for CO on metal oxides is fairly high[28,75,76]), yielding a lattice gas which gives rise to (1×1) diffraction peaks only. In order to test this hypothesis, we have carried out periodic DFT calculations for the activation barrier of diffusion for single CO molecules between neighboring lattice sites. On the DFT/PBE level we found no bound transition state. In particular, the CO/TiO_2 interaction was purely repulsive when a upright-oriented CO molecule was shifted from its fivefold coordinated Ti adsorption site to a bridging position between neighboring Ti surface atoms. Since van der Waals interactions are not captured in the DFT/PBE calculations, there is still the possibility of a weakly bound van der Waals transition state. However, based on the comparison of the results of our DFT/PBE, MP2, and SCS-MP2 calculations for the CO binding energy, we can conclude that the van der Waals interaction of CO with TiO_2 for distances around the CO/TiO_2 bond length is less than 100 meV. Thus, we can estimate that the barrier for diffusion of CO will be at least 0.26 eV and could be as much as the full desorption energy of 0.36 eV. Such fairly large values could well explain the absence of higher order commensurate CO overlayers at lower coverages.

We now turn to the question of the structure within the saturated CO layer on the TiO_2 surface. According to the results of the DFT calculations, this CO adlayer should show a (2×1) structure as indicated in Fig. 7. In this structure all CO molecules are adsorbed on all coordinatively unsaturated Ti ions in the top surface plane. In order to reduce the repulsion between the adjacent CO molecules, the CO axis is slightly tilted in alternating directions. Such an arrangement is, in fact, similar to the situation which is frequently found for CO bound on the (110) surfaces of fcc transition metals, e.g., Ni(110),[77] but also on ionic crystals like for CO/NaCl(001) (Ref. 78) or, as mentioned above, as a motive of a more complicated structure for CO/MgO(001).[4–6] Furthermore, the same zigzag tilt of the adsorbate molecules in order to reduce the repulsive interaction between molecules on neighboring lattice sites has been proposed by a detailed quantum-chemical study for the adsorption of N_2 on TiO_2(110).[79,80]

Such a (2×1) structure should in principle give rise to additional diffraction peaks along the [001] direction. The apparent inconsistency with the experimental data from He-atom diffraction where no such superstructure peak is observed is resolved by considering that the particular (2×1) structure proposed for the CO molecules in Fig. 8 [which is very similar to that observed for a saturated monolayer of CO adsorbed on Ni(110)[72,73]] contains a glide plane symmetry, which in turn leads to the extinction of every second diffraction peak.[65,81] Note that also a (2×2) structure with glide planes along both high-symmetry directions would be consistent with the absence of superstructure peaks, see Fig. 8. Taking into account the presence of glide planes, the He-atom diffraction scans recorded along this high-symmetry direction are thus in full accord with the structural model proposed on the basis of the theoretical calculations.

It is interesting to note that along the other high-symmetry direction $[1\bar{1}0]$, all the diffraction peaks are strongly broadened (see Fig. 2). This is surprising at first sight since the diffraction peaks in the other direction remain as sharp as those of the substrate peaks prior to adsorption of the CO molecules. This anisotropic broadening has been reproduced a number of times for different TiO_2 specimens. A similar anisotropic broadening has been observed for other adsorbate adlayers on substrates with twofold symmetry. For example, in the cases of N_2 adsorbed on Ni(110), the difference in the order parameter for the two orthogonal high-symmetry direction leads to rather elongated diffraction spots, i.e., the full width at half maximum (FWHM) of the spots is strongly different for the two different high-symmetry directions.[82] In the present case sharp diffraction peaks (i.e., small FWHM values) are only seen along the [001] direction, thus demonstrating the presence of a high degree of lateral order along this crystal axis. The large FWHM value of the diffraction peaks along the other direction, $[1\bar{1}0]$, reveals the presence of short-range order only, similar to the case of N_2 adsorbed on Ni(110). The periodic

Downloaded 03 Nov 2010 to 134.147.252.238. Redistribution subject to AIP license or copyright; see http://jcp.aip.org/about/rights_and_permissions

DFT/PBE calculations have shown that a shift of the tilted CO molecules by one substrate lattice constant between neighboring rows (i.e., introduction of a translational domain boundary) leads only to a negligible change in energy. As a result, a high density of such domain boundaries has to be expected. A schematic model for this scenario is shown in Fig. 8. The presence of such domain boundaries running perpendicular to the $[1\bar{1}0]$ will lead to a reduction in lateral order along this direction but not along [001]. Accordingly, the diffraction peaks will show an anisotropic shape, with a small FWHM along [001], where the lateral order is not affected by the introduction of the domain boundaries, and a large FWHM along the $[1\bar{1}0]$ direction. On the basis of these considerations we conclude that the anisotropy seen in the FWHM of the diffraction peaks is fully consistent with the presence of a (2×1) CO superstructure as predicted by theory.

VI. CONCLUSIONS

We have presented a detailed and comprehensive analysis of the adsorption of CO on the ideal terraces of the rutile $TiO_2(110)$ surface using a number of different experimental methods, He atom scattering, HREELS, and TDS, as well as two different theoretical approaches. It is found that at temperatures below 70 K, exposure to CO leads to the adsorption of a full CO monolayer and the formation of an ordered (2×1) superstructure with a glide symmetry plane similar to the geometry of densely packed CO adlayers on Ni(110).[72,73] The CO molecules are tilted out of their perpendicular orientation and form zigzag lines along the [001] direction in order to reduce their repulsive interactions. The lateral repulsion between adjacent CO molecules along the [001] directions leads to the desorption of half of the CO molecules above 70 K and the formation of a disordered adsorbate layer due to a limited surface diffusion. First-principles calculations and a detailed analysis of the conventional TDS data considering the CO–CO repulsion yield binding energies of 0.36 eV for single CO molecules and 0.20 eV at full monolayer coverage, corresponding to a repulsion energy of 0.16 eV. No indications for a significant CO–CO repulsion beyond the nearest-neighbor distance are found. CO molecules desorbing in a high temperature TDS tail between 150 and 170 K with a binding energy of 0.43/0.44 eV reported in previous work[26–28] are, on the basis of the present TDS data recorded for defective TiO_2 surfaces, assigned to CO molecules bound to defects such as step edges and vacancies. The HREEL spectra show a CO stretching mode at 273 meV (2200 cm^{-1}), strongly indicating that CO is bound via the carbon atom to the fivefold coordinated Ti sites. The results of our theoretical calculations for the binding energy, the repulsion between adjacent CO molecules, and the CO stretch frequency are in excellent agreement with the experimental findings.

ACKNOWLEDGMENTS

The work reported here has been supported by the German Research Foundation (DFG) through the Collaborative Research Center SFB 558 "Metal-Substrate Interactions in Heterogeneous Catalysis." We thank Professor U. Burghaus (now at North Dakota State University, Fargo, USA) for help with some of the measurements. D.M. is grateful to Fonds der Chemischen Industrie (FCI) for general support, and H.Q. thanks the IMPRS of SurMat for a research grant. Computational resources were provided by BOVILAB@RUB (Bochum).

[1] H. Over, Prog. Surf. Sci. **58**, 249 (1998).
[2] J. L. Whitten and H. Yang, Surf. Sci. Rep. **24**, 55 (1996).
[3] M. Gajdoš, A. Eichler, and J. Hafner, J. Phys.: Condens. Matter **16**, 1141 (2004).
[4] R. Wichtendahl, M. Rodriguez-Rodrigo, U. Härtel, H. Kuhlenbeck, and H.-J. Freund, Phys. Status Solidi A **173**, 93 (1999).
[5] J. Heidberg, M. Kandel, D. Meine, and U. Wildt, Surf. Sci. **331–333**, 1467 (1995).
[6] R. Gerlach, A. Glebov, G. Lange, J. P. Toennies, and H. Weiss, Surf. Sci. **331–333**, 1490 (1995).
[7] Y. Wang, Z. Phys. Chem. **222**, 927 (2008).
[8] C. Rohmann, Y. Wang, M. Muhler, J. B. Metson, H. Idriss, and Ch. Wöll, Chem. Phys. Lett. **460**, 10 (2008).
[9] M. Kurtz, J. Strunk, O. Hinrichsen, M. Muhler, K. Fink, B. Meyer, and Ch. Wöll, Angew. Chem. **117**, 2850 (2005); Angew. Chem., Int. Ed. **44**, 2790 (2005).
[10] M. Haruta, J. Catal. **115**, 301 (1989).
[11] M. Haruta, J. Catal. **144**, 175 (1993).
[12] V. Staemmler, K. Fink, B. Meyer, D. Marx, M. Kunat, S. Gil Girol, U. Burghaus, and Ch. Wöll, Phys. Rev. Lett. **90**, 106102 (2003).
[13] B. Meyer and D. Marx, J. Phys.: Condens. Matter **15**, L89 (2003).
[14] S.-H. Shi, C. Shi, K. Fink, and V. Staemmler, Chem. Phys. **287**, 183 (2003).
[15] U. Diebold, Surf. Sci. Rep. **48**, 53 (2003).
[16] K. Tanaka and J. M. White, J. Phys. Chem. **86**, 4708 (1982).
[17] K. Tanaka and J. M. White, J. Catal. **79**, 81 (1983).
[18] G. Busca, H. Saussey, O. Saur, J. C. Lavalley, and V. Lorenzelli, Appl. Catal. **14**, 245 (1985).
[19] C. Morterra, E. Garrone, V. Bolis, and B. Fubini, Spectrochim. Acta, Part A **43**, 1577 (1987).
[20] C. Morterra, J. Chem. Soc., Faraday Trans. 1 **84**, 1617 (1988).
[21] K. Hadjiivanov, A. Davidov, and D. Klissurski, Kinet. Katal. **29**, 161 (1988).
[22] K. Hadjiivanov, J. Lamotte, and J.-C. Lavalley, Langmuir **13**, 3374 (1997).
[23] L. Ferretto and A. Glisenti, Chem. Mater. **15**, 1181 (2003).
[24] W. Göpel, G. Rocker, and R. Feierabend, Phys. Rev. B **28**, 3427 (1983).
[25] G. B. Raupp and J. A. Dumesic, J. Phys. Chem. **89**, 5240 (1985).
[26] A. Linsebigler, G. Lu, and J. T. Yates, Jr., J. Chem. Phys. **103**, 9438 (1995).
[27] A. Linsebigler, G. Lu, and J. T. Yates, Jr., J. Phys. Chem. **100**, 6631 (1996).
[28] Z. Dohnálek, J. Kim, O. Bondarchuk, J. M. White, and B. D. Kay, J. Phys. Chem. B **110**, 6229 (2006).
[29] H. Kobayashi and M. Yamaguchi, Surf. Sci. **214**, 466 (1989).
[30] A. Fahmi and C. Minot, J. Organomet. Chem. **478**, 67 (1994).
[31] G. Pacchioni, A. M. Ferrari, and P. S. Bagus, Surf. Sci. **350**, 159 (1996).
[32] P. Reinhardt, M. Causá, C. M. Marian, and B. A. Heß, Phys. Rev. B **54**, 14812 (1996).
[33] D. C. Sorescu and J. T. Yates, Jr., J. Phys. Chem. B **102**, 4556 (1998).
[34] M. Casarin, C. Maccato, and A. Vittadini, J. Phys. Chem. B **102**, 10745 (1998).
[35] Z. Yang, R. Wu, Q. Zhang, and D. W. Goodman, Phys. Rev. B **63**, 045419 (2001).
[36] T. Bredow, L. Giordano, F. Cinquini, and G. Pacchioni, Phys. Rev. B **70**, 035419 (2004).
[37] R. Lindsay, A. Wander, A. Ernst, B. Montanari, G. Thornton, and N. M. Harrison, Phys. Rev. Lett. **94**, 246102 (2005).
[38] S. J. Thompson and S. P. Lewis, Phys. Rev. B **73**, 073403 (2006).
[39] P. M. Kowalski, B. Meyer, and D. Marx, Phys. Rev. B **79**, 115410 (2009).
[40] Ch. Wöll, J. Phys.: Condens. Matter **16**, S2981 (2004).
[41] F. Traeger, ChemPhysChem **7**, 1006 (2006).
[42] Ch. Wöll, Prog. Surf. Sci. **82**, 55 (2007).

Downloaded 03 Nov 2010 to 134.147.252.238. Redistribution subject to AIP license or copyright; see http://jcp.aip.org/about/rights_and_permissions

[43] E. A. Akhadov, S. A. Safron, J. G. Skofronick, D. H. Van Winkle, F. A. Flaherty, and R. Fatema, Phys. Rev. B **68**, 035409 (2003).
[44] F. Traeger, D. Langenberg, Y. K. Gao, and Ch. Wöll, Phys. Rev. B **76**, 033410 (2007).
[45] H.J. Kreuzer, S.H. Payne, ASTEK, A software package for the analysis and simulation of thermal equilibrum and kinetics of gases adsorbed on solid surfaces, Version 2.0, Helix Science Applications (618 Ketch Harbour Road, Portuguese Cove, N.S. 3V3 1K1, Canada), 1993–1995.
[46] H. Qiu, H. Idriss, Y. Wang, and Ch. Wöll, J. Phys. Chem. C **112**, 9828 (2008).
[47] Y. Wang and Ch. Wöll, "Chemical reactions on metal oxide surfaces investigated by vibrational spectroscopy," Surf. Sci. (to be published).
[48] B. J. Hinch, A. Lock, H. H. Madden, J. P. Toennies, and G. Witte, Phys. Rev. B **42**, 1547 (1990).
[49] Y. Wang, K. Jacobi, and G. Ertl, J. Phys. Chem. B **109**, 7883 (2005).
[50] S. Reiß, H. Krumm, A. Niklewski, V. Staemmler, and Ch. Wöll, J. Chem. Phys. **116**, 7704 (2002).
[51] J. Hutter *et al.*, CPMD program package, see www.cpmd.org.
[52] D. Marx and J. Hutter, in *Modern Methods and Algorithms of Quantum Chemistry*, edited by J. Grotendorst (NIC, FZ Jülich, 2000), p. 301; see www.theochem.rub.de/go/cprev.html.
[53] J. P. Perdew, K. Burke, and M. Ernzerhof, Phys. Rev. Lett. **77**, 3865 (1996); **78**, 1396E (1997).
[54] D. Vanderbilt, Phys. Rev. B **41**, 7892 (1990).
[55] S. C. Abrahams and J. L. Bernstein, J. Chem. Phys. **55**, 3206 (1971).
[56] A. Redondo, W. A. Goddard III, and T. C. McGill, Surf. Sci. **132**, 49 (1983).
[57] S. Grimme, J. Chem. Phys. **118**, 9095 (2003).
[58] P. Fuentealba, L. Vonszentpaly, H. Preuss, and H. Stoll, J. Phys. Chem. B **18**, 1287 (1985).
[59] F. Weigend, M. Haser, H. Patzelt, and R. Ahlrichs, Chem. Phys. Lett. **294**, 143 (1998).
[60] A. Schäfer, H. Horn, and R. Ahlrichs, J. Chem. Phys. **97**, 2571 (1992).
[61] S. F. Boys and F. Bernardi, Mol. Phys. **19**, 553 (1970).
[62] TURBOMOLE, a development of University of Karlsruhe and Forschungzentrum Karlsruhe GmbH, 1989–2007, TURBOMOLE GmbH, 2007; available from http://www.turbomole.com.
[63] C. Hättig, A. Hellweg, and A. Köhn, Phys. Chem. Chem. Phys. **8**, 1159 (2006).
[64] M. Kunat, U. Burghaus, and Ch. Wöll, Phys. Chem. Chem. Phys. **6**, 4203 (2004).
[65] R. M. Lambert, Surf. Sci. **49**, 325 (1975).
[66] M. Kunat and U. Burghaus, Surf. Sci. **544**, 170 (2003).
[67] J. Libuda and G. Scoles, J. Phys. Chem. B **103**, 9933 (1999).
[68] P. A. Redhead, Vacuum **12**, 203 (1962).
[69] K. L. D'Amico, F. R. McFeely, and E. I. Solomon, J. Am. Chem. Soc. **105**, 6380 (1983).
[70] Y. Wang, B. Meyer, X. Yin, M. Kunat, D. Langenberg, F. Traeger, A. Birkner, and Ch. Wöll, Phys. Rev. Lett. **95**, 266104 (2005).
[71] Y. Wang, X. Xia, A. Urban, H. Qiu, J. Strunk, B. Meyer, Ch. Wöll, and M. Muhler, Angew. Chem. **119**, 7456 (2007); Angew. Chem., Int. Ed. **46**, 7315 (2007).
[72] H. Kuhlenbeck, M. Neumann, and H.-J. Freund, Surf. Sci. **173**, 194 (1986).
[73] H. Kuhlenbeck, H. B. Saalfeld, U. Buskotte, M. Neumann, H.-J. Freund, and E. W. Plummer, Phys. Rev. B **39**, 3475 (1989).
[74] T. Helgaker, P. Jørgensen, and J. Olsen (*Molecular Electronic-Structure Theory* (Wiley, New York, 2000).
[75] T. Becker, C. Boas, U. Burghaus, and Ch. Wöll, Phys. Rev. B **61**, 4538 (2000).
[76] M. Kunat, C. Boas, T. Becker, U. Burghaus, and Ch. Wöll, Surf. Sci. **474**, 114 (2001).
[77] C. W. Bauschlicher, Chem. Phys. Lett. **115**, 535 (1985).
[78] N.-T. Vu, A. Jakalian, and D. B. Jack, J. Chem. Phys. **106**, 2551 (1997).
[79] F. Rittner, R. Fink, B. Boddenberg, and V. Staemmler, Phys. Rev. B **57**, 4160 (1998).
[80] F. Rittner, B. Boddenberg, R. F. Fink, and V. Staemmler, Langmuir **15**, 1449 (1999).
[81] A. L. Glebov, V. Panella, J. P. Toennies, F. Traeger, H. Weiss, S. Picaud, P. N. M. Hoang, and C. Girardet, Phys. Rev. B **61**, 14028 (2000).
[82] M. Grunze, P. H. Kleban, and W. N. Unertl, Phys. Rev. Lett. **51**, 582 (1983).

Downloaded 03 Nov 2010 to 134.147.252.238. Redistribution subject to AIP license or copyright; see http://jcp.aip.org/about/rights_and_permissions